Letter

High-temperature fractional quantum Hall state in the Floquet kagome flat band

Hang Liu,[1,2,4,*] Gurjyot Sethi,[2,*] D. N. Sheng,[5] Yinong Zhou,[2] Jia-Tao Sun,[1,3,†] Sheng Meng,[1,4,‡] and Feng Liu[2,§]

[1]*Beijing National Laboratory for Condensed Matter Physics and Institute of Physics, Chinese Academy of Sciences, Beijing 100190, People's Republic of China*

[2]*Department of Materials Science and Engineering, University of Utah, Salt Lake City, Utah 84112, USA*

[3]*School of Information and Electronics, MIIT Key Laboratory for Low-Dimensional Quantum Structure and Devices, Beijing Institute of Technology, Beijing 100081, People's Republic of China*

[4]*Songshan Lake Materials Laboratory, Dongguan, Guangdong 523808, People's Republic of China*

[5]*Department of Physics and Astronomy, California State University, Northridge, California 91330, USA*

(Received 29 June 2021; revised 21 September 2021; accepted 8 April 2022; published 29 April 2022)

A fractional quantum Hall effect (FQHE) has been predicted in a topological flat band (FB) by a single-particle band structure combined with phenomenological theory or solution of a many-body lattice Hamiltonian with fuzzy parameters. A long-standing roadblock toward the realization of a FB-FQHE is lacking the many-body solution of specific materials under realistic conditions. We demonstrate a combined study of single-particle Floquet band theory with exact diagonalization (ED) of a many-body Hamiltonian. We show that a time-periodic circularly polarized laser inverts the sign of second-nearest-neighbor hopping in a kagome lattice and enhances spin-orbit coupling in one spin channel to produce a Floquet FB with a high flatness ratio of bandwidth over band gap, as exemplified in monolayer $Pt_3C_{36}S_{12}H_{12}$. The ED of the resultant Floquet-kagome lattice Hamiltonian gives a one-third-filling ground state with a laser-dependent excitation gap of a FQH state, up to an estimated temperature above 70 K. Our findings pave the way for exploring the alluding high-temperature FB-FQHE.

DOI: 10.1103/PhysRevB.105.L161108

Integer quantum Hall effect (IQHE) and fractional quantum Hall effect (FQHE) arising from intrinsic band topology in crystal lattices can potentially overcome the low temperature and high magnetic field required for their counterparts in two-dimensional (2D) electron gas [1–8]. The IQHE without Landau level (LL) was originally proposed by Haldane [9] in a honeycomb lattice model with a Chern insulating gap, and was recently predicted [10–12] and observed [13] in Chern insulators. Also, a partially filled Chern flat band (FB) in 2D lattices is predicted to support high-temperature FQHE [14–17]. A widely used numerical technique to identify the existence of FQHE in lattice systems is the exact diagonalization (ED) of a FB Hamiltonian with a many-body Hubbard interaction [17–22], where the signatures of Laughlin-like state [20–22], including ground-sate degeneracy, spectral flow, and fractional statistics, can be shown for a partially filled Chern FB.

Some 2D materials have been found to host FBs from first-principles calculations [23–32]; however, none of them has a sufficiently large flatness ratio of band gap (Δ) over band width (w)—i.e., $\Delta/w \gg 1$—which is required for realizing high-temperature FQHE [14–17]. It has been shown that to obtain an "isolated" FB with large Δ/w, a peculiar negative kinetic hopping integral and strong spin-orbit coupling (SOC) are needed in a kagome lattice [14]. But, such requirements are unlikely to be met with the natural decay of lattice hopping with interatomic spacing in real materials; and indeed, all the FBs found so far have too small a flatness ratio of $\Delta/w \sim 1$ [23–32]. On the other hand, the existing many-body ED calculations are carried out for FB–lattice models using artificial hopping parameters, SOC strength, and a Hubbard interaction [21,22], which are disconnected from realistic materials and conditions.

Therefore, there remain at least two challenges to demonstrating the FB-FQHE in the real world: first, developing an approach to tune the lattice hopping parameters so that they can meet the stringent requirements to attain a large Δ/w; and second, solving the many-body lattice Hamiltonian corresponding to real materials to show directly the solution of FQHE. In this letter, we demonstrate that the Floquet-FB in a kagome lattice can reach an unprecedented high $\Delta/w \gg 1$ through photo-engineered lattice interactions. A time-periodic circularly polarized laser (CPL) strongly alters the steady-state electronic interactions in a kagome lattice by virtual photon processes (VPPs), in particular to invert the second-nearest-neighbor (2NN) kinetic hopping and enhance the effective SOC in one spin channel locked with CPL helicity. Consequently, the originally dispersive Chern band is transformed into a FB. In a prototypical example of monolayer $Pt_3C_{36}S_{12}H_{12}$, an organometallic framework synthesized from reacting triphenylene hexathiol molecules (HTT) with $PtCl_2$, which is called HTT-Pt, the so-formed FB reaches a flatness ratio of $\Delta/w \sim 40$. Furthermore, we use the ED method to solve the material-specific lattice Hamiltonian of HTT-Pt under laser illumination, based on realistic Floquet hopping, SOC, and Hubbard interaction parameters. We show that the original electronic kagome lattice Hamiltonian *does*

*These two authors contributed equally to this work.
†jtsun@iphy.ac.cn
‡smeng@iphy.ac.cn
§fliu@eng.utah.edu

not support FQHE; only the Floquet-kagome lattice can host the FQH states at the one-third filling of a FB, with a many-body excitation gap tunable by laser intensity, reaching an estimated temperature above 70 K.

Recently, irradiating time-periodic light on crystals has been shown to offer an effective way to create and control the experimentally measurable Floquet topological electronic states [33–36], such as the nonequilibrium IQHE [37,38] and FQHE [39] closely related to the present study, Floquet-Dirac/Weyl semimetals [40–44], and topological FB positions [45,46]. Here, we illustrate an interesting case of a laser-created FB with large Δ/w for high-temperature FQHE.

To study coherent interactions between a laser field and a kagome lattice, we consider the NN (2NN) kinetic hopping integral $\gamma_1{}^0(\gamma_2{}^0)$ and SOC strength $\lambda_1{}^0(\lambda_2{}^0)$ in two spin channels $s = \pm 1$ (see details in Fig. S1 and Section I of the Supplemental Material [47]), and we adopt a CPL with a time-dependent vector potential $\boldsymbol{A}(t) = A_0(\eta\cos\omega t, \sin\omega t)$, where $\hbar\omega$, A_0, and η are photon energy, laser amplitude, and laser helicity, respectively. Under a time-periodic off-resonant CPL, the Floquet-Bloch Hamiltonian can be expanded as [38,52]

$$H_F(\boldsymbol{k}) = H_0(\boldsymbol{k}) + \sum_{n\in Z^+}\frac{1}{n\hbar\omega}[H_{-n}(\boldsymbol{k}), H_n(\boldsymbol{k})] + \mathrm{O}\left(\frac{1}{\omega^2}\right). \tag{1}$$

The VPPs, comprising the photon absorption ($n' \in Z^+$) and emission ($n' \in Z^-$) terms, $H_{n'}(\boldsymbol{k}) = \frac{1}{T}\int_0^T H(\boldsymbol{k},t)e^{in'\omega t}dt$, will modify ($\gamma_1$, λ_1) and (γ_2, λ_2) [Fig. 1(a)], derived as

$$\begin{aligned}\gamma_1 =& \gamma_1{}^0 J_0(A_1) + s\eta\{2J_1(A_1)[\sqrt{3}J_1(A_1)B_1 + J_1(A_2)C_1] \\ &+ \sqrt{3}J_2(A_1)\cdot[J_2(A_1)B_1 + J_2(A_2)C_1]\}/(\hbar\omega),\end{aligned} \tag{2}$$

$$\begin{aligned}\lambda_1 =& \lambda_1{}^0 J_0(A_1) + s\eta\{J_1(A_1)[\sqrt{3}J_1(A_1)D_1 - 2J_1(A_2)C_2] \\ &+ \sqrt{3}J_2(A_1)[J_2(A_1)D_1/2 - J_2(A_2)C_2]\}/(\hbar\omega),\end{aligned} \tag{3}$$

$$\begin{aligned}\gamma_2 =& \gamma_2{}^0 J_0(A_2) - \sqrt{3}s\eta\big\{2\big[J_1^2(A_1)B_1 + J_1^2(A_2)B_2\big] \\ &- \big[J_2^2(A_1)B_1 - J_2^2(A_2)B_2\big]\big\}/(\hbar\omega),\end{aligned} \tag{4}$$

and

$$\begin{aligned}\lambda_2 =& \lambda_2{}^0 J_0(A_2) + \sqrt{3}s\eta\big\{\big[J_1^2(A_1)D_1 - J_1^2(A_2)D_2\big] \\ &- \big[J_2^2(A_1)D_1 + J_2^2(A_2)D_2\big]/2\big\}/(\hbar\omega),\end{aligned} \tag{5}$$

where $A_1 = aeA_0/2\hbar$ (a is lattice constant), $A_2 = \sqrt{3}A_1$, $B_1 = \gamma_1{}^0\lambda_1{}^0$, $B_2 = \gamma_2{}^0\lambda_2{}^0$, $C_1 = \gamma_1{}^0\lambda_2{}^0 - \gamma_2{}^0\lambda_1{}^0$, $C_2 = \gamma_1{}^0\gamma_2{}^0 + \lambda_1{}^0\lambda_2{}^0$, and $D_1 = (\gamma_1{}^0)^2 - (\lambda_1{}^0)^2$, $D_2 = (\gamma_2{}^0)^2 - (\lambda_2{}^0)^2$. J_m is the first kind of Bessel function with an order of $m = 0, 1, 2$, which comes from the m-order VPP in Eq. (1). For high-frequency driving, the first-order term ($\sim\omega^{-1}$) dominates the Floquet band structure so that the higher-order terms can be neglected (Supplemental Material Fig. S2 [47]) [35,40,52].

By chiral symmetry, the effect of a left-handed CPL ($\eta = 1$) on spin-up ($s = 1$) bands is the same as that of a right-handed CPL ($\eta = -1$) on spin-down ($s = -1$) bands. Thus, here we focus on the case of $\eta = 1$ and $s = 1$. To illustrate photo-engineered interactions and the resulting Floquet-kagome band structure, we choose a prototypical example with tight binding hopping integrals of $\gamma_1{}^0 = 48$ meV, $\lambda_1{}^0 = 0.180\gamma_1{}^0$, $\gamma_2{}^0 = 0.112\gamma_1{}^0$, and $\lambda_2{}^0 = 0.038\gamma_1{}^0$, which are fitted from the first-principles band structure of monolayer HTT-Pt (Supplemental Material Fig. S3 and Section II in Supplemental Material [47]) [30,31,53]. Applying a CPL with $\hbar\omega = 8.0\gamma_1{}^0$, γ_2 decreases with the increasing A_0, as shown in Fig. 1(b). Beyond $A_0 = 476$ V/c (corresponding to 0.039 V/Å or 2.0×10^{10} W/cm^2), γ_2 is inverted from positive to negative, which is essential to flatten the bottom Chern band (see details in Supplemental Material Fig. S4 [47]). At the same time, both λ_1 and λ_2 increase with A_0 [Fig. 1(b)], which is critical to increase Δ/w. In sharp contrast to equilibrium kagome materials, the Floquet-kagome hopping integrals no longer decay exponentially with the interatomic distance and can have different phases (signs).

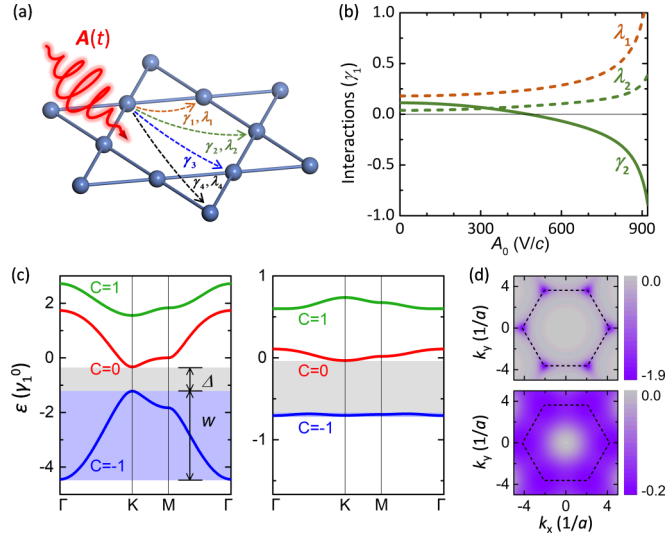

FIG. 1. Photo-engineered kagome interactions and Floquet bands. (a) Schematic illustration of lattice hopping driven by a time-periodic CPL. γ_1 (λ_1), γ_2 (λ_2), γ_3, and γ_4 (λ_4) represent the NN, 2NN, 3NN, and 4NN kinetic (SOC) hopping, respectively. (b) Evolution of λ_1, γ_2, and λ_2 versus laser amplitude A_0 for spin-up bands in monolayer HTT-Pt under a CPL with $\hbar\omega = 8\gamma_1{}^0$ and $\eta = 1$. (c) Left panel: Kagome bands in equilibrium. Right panel: Floquet-kagome bands induced by a CPL with $A_0 = 800$ V/c in (b). (d) Top panel: The Berry curvature Ω for the bottom dispersive Chern band with $\Delta/w \sim 0.27$ in the left panel of (c). The dashed lines mark the FBZ. Bottom panel: The laser-driven Ω of the bottom FB with $\Delta/w \sim 29$ in the right panel of (c).

The unusual photo-engineered interactions in Fig. 1(b)—i.e., inverting the 2NN kinetic hopping and enhancing the SOC in one spin channel locked with laser helicity—lead to an intriguing evolution of Floquet-Kagome bands. The equilibrium spin-up bands have a direct SOC gap $\Delta = 0.887\gamma_1{}^0$, separating the bottom Chern band ($C = -1$) from the middle Dirac band ($C = 0$) [left panel in Fig. 1(c)]. The bottom Chern band has a sizable width $w = 3.228\gamma_1{}^0$ and a small flatness ratio $\Delta/w = 0.27$. The CPL significantly reduces its width, such as to $w = 0.022\gamma_1{}^0$ with $A_0 = 800$ V/c, which is ~150 times narrower than its equilibrium value, as shown in the right panel of Fig. 1(c). Also, it becomes well separated from the band above by a large SOC gap

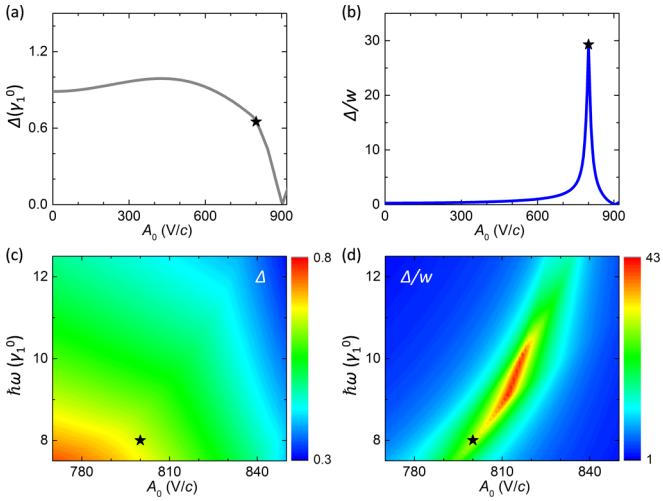

FIG. 2. Evolution of (a) spin-up band gap Δ and (b) flatness ratio Δ/w versus laser intensity produced for HTT-Pt under CPL with $\hbar\omega = 8{\gamma_1}^0$. (c, d) Phase diagram of Δ and Δ/w in the parameter space of $\hbar\omega$ and A_0. The star marks the specific case with $\Delta/w \sim 29$ shown in the right panel of Fig. 1(c), as used for the ED study.

$\Delta = 0.650{\gamma_1}^0$. Consequently, an unprecedented high value of $\Delta/w \sim 29$ is achieved. The nonmonotonic dependence of Δ/w on A_0, peaking at $A_0 = 800$ V/c for $\hbar\omega = 8{\gamma_1}^0$, can be better understood by analyzing simplified models with only NN equilibrium hopping integrals, and evaluating the detailed dependence of Δ, w, and Δ/w on laser-driven hopping integrals (Supplemental Material Section IV and Figs. S4 and S5 [47]). The spin-down Floquet bands evolve differently—e.g., exhibiting bands with a high Chern number (Supplemental Material Fig. S6 [47]). With a spontaneous Zeeman splitting of $M = -2{\gamma_1}^0$ induced by a partially filled FB [23,30], the spin-up and -down Floquet bands of monolayer HTT-Pt can be fully separated from each other (Supplemental Material Fig. S7 [47]).

We have analyzed the laser-driven distribution of Berry curvature (Ω) of the photo-flattened Chern band to identify essential features for realizing FQHE. At equilibrium, Ω of the bottom dispersive Chern band is highly localized at the K and K' points of the first Brillouin zone (FBZ) [top panel in Fig. 1(d)], which is characterized by a large mean-square deviation of $\langle(\Delta\Omega)^2\rangle = 7.2 \times 10^{-2}$ [54]. Differently, Ω of the ultraflat and isolated bottom Floquet-Chern band becomes delocalized in the whole FBZ [bottom panel in Fig. 1(d)], characterized by $\langle(\Delta\Omega)^2\rangle = 3.9 \times 10^{-3}$. The uniform distribution of Berry curvature in a FB indicates a very short magnetic length l on the order of lattice constant [14], in analogy to a LL, which favors FQHE with a large excitation gap and high temperature [8,55] (see Supplemental Material Section V [47]).

To identify the optimal laser intensity and photon energy for maximizing the band gap and flatness ratio, we have mapped out Δ and Δ/w as functions of $\hbar\omega$ and A_0. Figure 2(a) and (b) shows their dependence on A_0 for a chosen $\hbar\omega = 8{\gamma_1}^0$. A maximum $\Delta/w \sim 29$ (also a large $\Delta = 0.650{\gamma_1}^0$) is reached at $A_0 = 800$ V/c. Figure 2(c) and (d) shows the phase diagrams of Δ and Δ/w in the parameter space of $\hbar\omega$ and A_0. There exists a large experimentally accessible parameter space to achieve a Chern FB with $\Delta > 0.54{\gamma_1}^0$ and $\Delta/w > 10$. In general, as the photon energy increases, the required laser intensity is stronger in order to create the desired band structure, because of an inverse linear scaling between the intensity of VPP and photon energy [Eq. (1)]. With $\hbar\omega = 9.1{\gamma_1}^0$ and $A_0 = 812$ V/c, a maximum $\Delta/w \sim 43$ is achieved, with a large $\Delta = 0.60{\gamma_1}^0$ (Supplemental Material Fig. S8 [47]).

Next, we investigate the possible existence of FQHE and assess its temperature in a specific material under realistic conditions by performing a series of ED studies of a kagome lattice with Floquet hopping parameters corresponding to HTT-Pt under laser illumination. The many-body Hamiltonian is $\hat{H} = \hat{H}_F + U\sum_{\langle i,j\rangle}\hat{n}_i\hat{n}_j$, where $\hat{H}_F$ is the HTT-Pt-specific Floquet-kagome Hamiltonian with ${\gamma_1}^0 \sim 0.048$ eV, $\hat{n}_j$ is the on-site particle number operator, and $U \sim 0.14$ eV ($3{\gamma_1}^0$) is the NN Hubbard repulsion (see details in Supplemental Material Section VI [47]). We note that in HTT-Pt, U is larger than the single-particle band gap (Δ). Because the two lower bands have, respectively, Chern number -1 and 0, any mixing between them will not change the Chern number of the lowest FB with band width w [19]. Hence, if $U \gg w$, interactions dominate and partial filling of the FB leads to a strongly correlated state, such as a FQH state. So, we exactly diagonalize the many-body Hamiltonian projected to the lowest FB for a finite system with $N_x \times N_y$ unit cells (Total sites $= 3 \times N_x \times N_y$). The filling factor is equal to $\upsilon = \frac{N_e}{N_x \times N_y}$, where N_e is the number of electrons in the system. Under periodic boundary conditions, we implement translational symmetries and diagonalize the Hamiltonian in each momentum sector $q = (2\pi k_x/L_x, 2\pi k_y/L_y)$, with k_x and k_y being the integers.

For comparison, we first calculated the energy spectra for the one-third filling of a 4×6 system for the equilibrium lattice, as shown in Fig. 3(a). There is no clear gap or the celebrated 3-fold degeneracy of a ground state [17–22], or any other identifiable signature of a one-third FQH state. This indicates that HTT-Pt by itself does not support FQHE. We then calculated the energy spectra for the Floquet lattices with different laser energies and intensities. One typical example is shown in Fig. 3(b) with $\hbar\omega = 8.0{\gamma_1}^0$, $A_0 = 800$ V/c. One notices a clear gap separating the 3-fold degenerate ground-state manifold from the excited states. Due to finite size effects, the degeneracy of the ground state is slightly lifted, but the energy spread is much smaller than the gap. Also, if one state in the ground-state manifold lies in the momentum sector (k_1, k_2), the next state can be always found at $(k_1 + N_e, k_2 + N_e)$ [modulo (N_x, N_y)]. This correlation implies that the ground state has a nontrivial topology [18,20]. The key features of finite gap and ground-state degeneracy have been checked for convergence with respect to system size (see Supplemental Material Fig. S9 [47]).

To ascertain further that the ground state is nontrivial, we also calculated the spectral flow [Fig. 3(c)] under a twisted boundary condition that is equivalent to the insertion of magnetic flux. According to Laughlin's gauge argument, if one adiabatically inserts three quantum fluxes into the one-third-filling FQH state, the states should evolve back to their original configuration [2]. This can be clearly seen in Fig. 3(c)

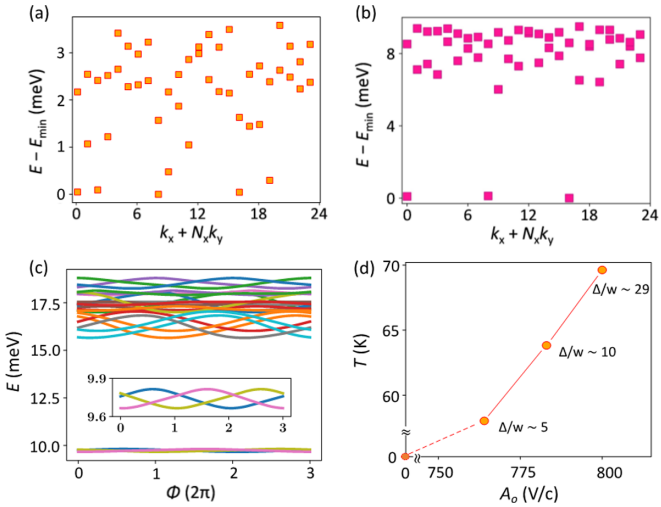

FIG. 3. ED solution of the Floquet FB-FHQE in HTT-Pt at $U = 3{\gamma_1}^0$. (a) Low-energy spectrum of $N_e = 8$ electrons in the equilibrium lattice with 4×6 kagome unit cells. (b) Low-energy spectrum of $N_e = 8$ electrons in the same lattice as in (a) driven by CPL with $A_0 = 800$ V/c, $\hbar\omega = 8{\gamma_1}^0$. (c) Spectral flow spectrum: evolution of (b) under the flux insertion along y direction. (d) Temperature estimated by the many-body gap of the one-third FQH state versus A_0.

for the three states in the ground-state manifold. There is no mixing between them and the excited states throughout the flux insertion. Thus, these states share a total Chern number of 1, giving a quantized Hall conductance of $\sigma_H = \frac{1}{3}\frac{e^2}{h}$ [56].

The many-body gap is $\Delta_{\rm ED} \sim 6$ meV [Fig. 3(b)], as calculated for the Floquet-kagome lattice using $\hbar\omega = 8.0{\gamma_1}^0$, $A_0 = 800$ V/c, and $U = 3{\gamma_1}^0$. Taking this Δ_{ED} as a rough estimate of critical temperature (T_c) for FB-FQHE, we obtain $T_c \sim$70 K [14,47]. In Fig. 3(d), we show that T_c increases monotonically with the increasing laser amplitude. We have calculated Δ_{ED} as a function U at a fixed laser intensity of $A_0 = 800$ V/c (i.e., fixed lattice hopping) and found $\Delta_{ED} = 0.042\,U$ (Supplemental Material Fig. S10 [47]), which is qualitatively the same but quantitatively about half of the empirical formula $\Delta_{\rm FQHE} = 0.09\,U$ [14] for LLs. In addition, we calculated Δ_{ED} as a function of kinetic lattice hopping (γ_1) for constant U and found $\Delta_{ED} = 0.03\,({\gamma_1}^0)^2/\gamma_1$ (Supplemental Material Fig. S10 [47]). This leads to a combined expression, $\Delta_{ED} = 0.01(U/\gamma_1){\gamma_1}^0$, showing the dependence of Δ_{ED} on both U and γ_1. It points to the apparent difference between FB-FQHE and LL-FQHE, as the former arises from a lattice system while the latter is lattice free.

In addition, we have verified the fractional exclusion statistics in the Floquet FB, which is another key characteristic of the FQH state in LLs [57]. In Fig. 4(a), we show the calculated quasihole excitation spectrum for the case of Fig. 3(b). This is done by keeping N_e fixed and by varying N_x and/or N_y to introduce a hole. The counting of the number of states below the gap in the quasihole spectrum must correspond to the counting given by the (1,3)-admissible rule based on the generalized Pauli principle [21],

$$N_{FQH}^{N_e} = N_x N_y \frac{(N_x N_y - 2N_e - 1)!}{N_e!(N_x N_y - 3N_e)!}. \quad (6)$$

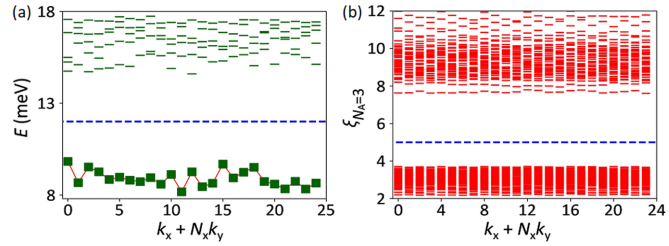

FIG. 4. Fractional statistics for the one-third FQH state as in Fig. 3. (a) Low-energy spectrum of eight electrons in the cluster with 5×5 kagome cells (equivalent to quasihole excitation of eight electrons in 4×6 Kagome cells). (b) PES probing a group of $N_A = 3$ electrons in Fig. 3(b).

As an example, we performed this calculation for eight electrons in a 5×5 lattice. The number of states below the gap is 25, in exact agreement with the (1,3)-admissible rule.

Moreover, to rule out other possible ground states, such as the Wigner crystal state, we calculated the particle-cut entanglement spectrum (PES). By partitioning N_e into two groups of N_A and N_B, and tracing out the degrees of freedom for N_B, we calculate the reduced density matrix $\rho_A = {\rm Tr}_B \sum_i |\phi_i\rangle\langle\phi_i|$, where the sum is over the three states in the ground-state manifold and $|\phi_i\rangle$ is their respective many-body wavefunctions. The eigenvalues of this matrix are given by $e^{-\xi}$ [21,58], and the entanglement energy levels ξ can then be displayed in groups labeled by the momentum (k_1, k_2) of N_A particles. In Fig. 4(b), we plot the PES for $N_A = 3$ in a 4×6 lattice. A clear entanglement gap can be seen, and the number of states below the gap matches exactly the quasihole counting for three particles in a 4×6 lattice, indicating a FQH state [21,22,58]. Besides $A_0 = 800$ V/c, the one-third fractional Hall conductance and key characteristics of the predicted FQHE are also demonstrated for other laser amplitudes (see Supplemental Material Figs. S11 and S12 [47]).

To facilitate a direct comparison with experimental measurement of Floquet states [34,36,59–61], we simulated time- and angle-resolved photo-electron spectroscopy, by adopting the experimental pump-probe scheme (see Supplemental Material Section VII and Fig. S13 [47]). The simulation shows there are ~5% electrons photo-excited from the bottom Floquet FB (Supplemental Material Fig. S13 [47]) to form Floquet dressed states through VPPs, which would result in a conductivity plateau of IQHE deviating from an exact integer (similar to that in Floquet graphene [36]), when the Fermi level lies in the gap above the bottom Floquet FB. Interestingly, however, this may not affect the FQHE measurement, because FQHE corresponds to the many-body ground state that occurs at exact one-third FB occupation, usually achieved by gating to tune the chemical potential. The laser intensity and energy for achieving reasonably large Δ/w corresponds to an electric field of $\sim 1 \times 10^8$ V/m, in the same range as experiments where the materials remain stable [34,36,59–61].

In summary, we have carried out a comprehensive study of FQHE in topological FB in specific materials under realistic conditions, by combining single-particle Floquet band theory with exact diagonalization of a many-body Hamiltonian. We conclude that the naturally existing electronic materials

are unlikely to support the FQHE because of a FB flatness ratio that is too small. We propose one viable approach to increase the flatness ratio is by Floquet band engineering via photo-inverted lattice hopping coupled with photo-enhanced SOC interaction. Using monolayer HTT-Pt as a prototypical example, we show that a Floquet-kagome lattice may exhibit a one-third-filling FB-FQHE above the liquid nitrogen temperature.

We thank Yongshi Wu, Tao Xiang, Zhiqiang Wang, Zheng Liu, and Xuanyu Long for helpful discussions. H. L., J.- T. S., and S. M. acknowledge financial support from the National Key Research and Development Program of China (Grants No. 2020YFA0308800 and No. 2016YFA0300902), the National Basic Research Program of China (Grant No. 2015CB921001), the National Natural Science Foundation of China (Grants No. 91850120, No. 11774396, No. 11974045, and No. 12147136), the Strategic Priority Research Program (B) of Chinese Academy of Sciences (Grant No. XDB30000000), the China Postdoctoral Science Foundation (Grant No. 2021M700163), the Guangdong Basic and Applied Basic Research Foundation (Grant No. 2021A1515110466), and the China Scholarship Council. G. S., Y. Z., and F. L. acknowledge support by the U.S. Department of Energy–Basic Energy Sciences (DOE-BES; Grant No. DE-FG02-04ER46148). D. N. S. acknowledges support by the U.S. DOE-BES (Grant No. DE-FG02-06ER46305). H. L., J.- T. S., and S. M. thank the Tianjin Supercomputing Center and the Platform for Data-Driven Computational Materials Discovery in Songshan Lake Materials Laboratory for providing the computing resources. G. S. and F. L. thank the Center for High Performance Computing at the University of Utah and the U.S. DOE–National Energy Research Scientific Computing Center.

[1] K. v. Klitzing, G. Dorda, and M. Pepper, New Method for High-Accuracy Determination of the Fine-Structure Constant Based on Quantized Hall Resistance, Phys. Rev. Lett. **45**, 494 (1980).

[2] R. B. Laughlin, Quantized Hall conductivity in two dimensions, Phys. Rev. B **23**, 5632 (1981).

[3] D. C. Tsui, H. L. Stormer, and A. C. Gossard, Two-Dimensional Magnetotransport in the Extreme Quantum Limit, Phys. Rev. Lett. **48**, 1559 (1982).

[4] F. D. M. Haldane, Fractional Quantization of the Hall Effect: A Hierarchy of Incompressible Quantum Fluid States, Phys. Rev. Lett. **51**, 605 (1983).

[5] R. B. Laughlin, Anomalous Quantum Hall Effect: An Incompressible Quantum Fluid with Fractionally Charged Excitations, Phys. Rev. Lett. **50**, 1395 (1983).

[6] D. Yoshioka, B. I. Halperin, and P. A. Lee, Ground State of Two-Dimensional Electrons in Strong Magnetic Fields and 1/3 Quantized Hall Effect, Phys. Rev. Lett. **50**, 1219 (1983).

[7] K. v. Klitzing, The quantized Hall effect, Rev. Mod. Phys. **58**, 519 (1986).

[8] R. L. Willett, H. L. Stormer, D. C. Tsui, A. C. Gossard, and J. H. English, Quantitative experimental test for the theoretical gap energies in the fractional quantum Hall effect, Phys. Rev. B **37**, 8476 (1988).

[9] F. D. Haldane, Model for a Quantum Hall Effect without Landau Levels: Condensed-Matter Realization of the "Parity Anomaly, Phys. Rev. Lett. **61**, 2015 (1988).

[10] C. X. Liu, X. L. Qi, X. Dai, Z. Fang, and S. C. Zhang, Quantum Anomalous Hall Effect in Hg(1-y)Mn(y)Te Quantum Wells, Phys. Rev. Lett. **101**, 146802 (2008).

[11] R. Yu, W. Zhang, H.- J. Zhang, S.- C. Zhang, X. Dai, and Z. Fang, Quantized anomalous Hall effect in magnetic topological insulators, Science **329**, 61 (2010).

[12] H. Liu, J. T. Sun, M. Liu, and S. Meng, Screening magnetic two-dimensional atomic crystals with nontrivial electronic topology, J. Phys. Chem. Lett. **9**, 6709 (2018).

[13] C.- Z. Chang *et al.*, Experimental observation of the quantum anomalous Hall effect in a magnetic topological insulator, Science **340**, 167 (2013).

[14] E. Tang, J. W. Mei, and X. G. Wen, High-Temperature Fractional Quantum Hall States, Phys. Rev. Lett. **106**, 236802 (2011).

[15] K. Sun, Z. Gu, H. Katsura, and S. Das Sarma, Nearly Flatbands with Nontrivial Topology, Phys. Rev. Lett. **106**, 236803 (2011).

[16] H. Katsura, I. Maruyama, A. Tanaka, and H. Tasaki, Ferromagnetism in the Hubbard model with topological/non-topological flat bands, Europhys. Lett. **91**, 57007 (2010).

[17] T. Neupert, L. Santos, C. Chamon, and C. Mudry, Fractional Quantum Hall States at Zero Magnetic Field, Phys. Rev. Lett. **106**, 236804 (2011).

[18] D. N. Sheng, Z. C. Gu, K. Sun, and L. Sheng, Fractional quantum Hall effect in the absence of Landau levels, Nat. Commun. **2**, 389 (2011).

[19] W. Li, Z. Liu, Y.- S. Wu, and Y. Chen, Exotic fractional topological states in a two-dimensional organometallic material, Phys. Rev. B **89**, 125411 (2014).

[20] E. J. Bergholtz and Z. Liu, Topological flat band models and fractional Chern insulators, Int. J. Mod. Phys. B **27**, 1330017 (2013).

[21] N. Regnault and B. A. Bernevig, Fractional Chern Insulator, Phys. Rev. X **1**, 021014 (2011).

[22] Y.- L. Wu, B. A. Bernevig, and N. Regnault, Zoology of fractional Chern insulators, Phys. Rev. B **85**, 075116 (2012).

[23] Z. Liu, Z. F. Wang, J. W. Mei, Y. S. Wu, and F. Liu, Flat Chern Band in a Two-Dimensional Organometallic Framework, Phys. Rev. Lett. **110**, 106804 (2013).

[24] Z. F. Wang, N. Su, and F. Liu, Prediction of a two-dimensional organic topological insulator, Nano Lett. **13**, 2842 (2013).

[25] M. Zhou, Z. Liu, W. Ming, Z. Wang, and F. Liu, Sd(2) Graphene: Kagome Band in a Hexagonal Lattice, Phys. Rev. Lett. **113**, 236802 (2014).

[26] X. Zhang and M. Zhao, Robust half-metallicity and topological aspects in two-dimensional Cu-TPyB, Sci. Rep. **5**, 14098 (2015).

[27] O. J. Silveira, S. S. Alexandre, and H. Chacham, Electron states of 2D metal–organic and covalent–organic honeycomb frameworks: ab initio results and a general fitting Hamiltonian, J. Phys. Chem. C **120**, 19796 (2016).

[28] M. G. Yamada, T. Soejima, N. Tsuji, D. Hirai, M. Dincă, and H. Aoki, First-principles design of a half-filled flat band of the kagome lattice in two-dimensional metal-organic frameworks, Phys. Rev. B **94**, 081102(R) (2016).

[29] L. Z. Zhang, Z. F. Wang, B. Huang, B. Cui, Z. Wang, S. X. Du, H. J. Gao, and F. Liu, Intrinsic two-dimensional organic topological insulators in metal-dicyanoanthracene lattices, Nano Lett. **16**, 2072 (2016).

[30] X. Zhang, Z. Wang, M. Zhao, and F. Liu, Tunable topological states in electron-doped HTT-Pt, Phys. Rev. B **93**, 165401 (2016).

[31] O. J. Silveira and H. Chacham, Electronic and spin-orbit properties of the kagome MOF family M3(1,2,5,6,9, 10-triphenylenehexathiol)2 (M = Ni, Pt, Cu and Au), J. Phys. Condens. Matter **29**, 09LT01 (2017).

[32] Z. Li, J. Zhuang, L. Wang, H. Feng, Q. Gao, X. Xu, W. Hao, X. Wang, C. Zhang, K. Wu, S. X. Dou, L. Chen, Z. Hu, and Y. Du, Realization of flat band with possible nontrivial topology in electronic Kagome lattice, Sci. Adv. **4**, eaau4511 (2018).

[33] T. Oka and S. Kitamura, Floquet engineering of quantum materials, Annu. Rev. Condens. Matter Phys. **10**, 387 (2019).

[34] Y. H. Wang, H. Steinberg, P. Jarillo-Herrero, and N. Gedik, Observation of Floquet-Bloch states on the surface of a topological insulator, Science **342**, 453 (2013).

[35] Z. F. Wang, Z. Liu, J. Yang, and F. Liu, Light-Induced Type-II Band Inversion and Quantum Anomalous Hall State in Monolayer FeSe, Phys. Rev. Lett. **120**, 156406 (2018).

[36] J. W. McIver, B. Schulte, F. U. Stein, T. Matsuyama, G. Jotzu, G. Meier, and A. Cavalleri, Light-induced anomalous Hall effect in graphene, Nat. Phys. **16**, 38 (2020).

[37] T. Oka and H. Aoki, Photovoltaic Hall effect in graphene, Phys. Rev. B **79**, 081406(R) (2009).

[38] T. Kitagawa, T. Oka, A. Brataas, L. Fu, and E. Demler, Transport properties of nonequilibrium systems under the application of light: Photoinduced quantum Hall insulators without Landau levels, Phys. Rev. B **84**, 235108 (2011).

[39] A. G. Grushin, A. Gomez-Leon, and T. Neupert, Floquet Fractional Chern Insulators, Phys. Rev. Lett. **112**, 156801 (2014).

[40] Z. Yan and Z. Wang, Tunable Weyl Points in Periodically Driven Nodal Line Semimetals, Phys. Rev. Lett. **117**, 087402 (2016).

[41] H. Liu, J.- T. Sun, C. Cheng, F. Liu, and S. Meng, Photoinduced Nonequilibrium Topological States in Strained Black Phosphorus, Phys. Rev. Lett. **120**, 237403 (2018).

[42] H. Liu, J.- T. Sun, C. Song, H. Huang, F. Liu, and S. Meng, Fermionic analogue of high temperature Hawking radiation in black phosphorus, Chin. Phys. Lett. **37**, 067101 (2020).

[43] H. Liu, J.- T. Sun, and S. Meng, Engineering Dirac states in graphene: Coexisting type-I and type-II Floquet-Dirac fermions, Phys. Rev. B **99**, 075121 (2019).

[44] H. Hubener, M. A. Sentef, U. De Giovannini, A. F. Kemper, and A. Rubio, Creating stable Floquet-Weyl semimetals by laser-driving of 3D Dirac materials, Nat. Commun. **8**, 13940 (2017).

[45] P. Roman-Taboada and G. G. Naumis, Topological flat bands in time-periodically driven uniaxial strained graphene nanoribbons, Phys. Rev. B **95**, 115440 (2017).

[46] L. Du, X. Zhou, and G. A. Fiete, Quadratic band touching points and flat bands in two-dimensional topological Floquet systems, Phys. Rev. B **95**, 035136 (2017).

[47] See Supplemental Material at http://link.aps.org/supplemental/10.1103/PhysRevB.105.L161108 for details about computational method, Floquet hopping equations and its phase diagram, kagome lattice, tight-binding fitting of monolayer HTT-Pt, calculation convergency, and Floquet spin-down band evolution, which includes Refs. [8,14,34,36,48–51,54,55,59–65].

[48] H. M. Guo and M. Franz, Topological insulator on the kagome lattice, Phys. Rev. B **80**, 113102 (2009).

[49] Z. Liu, F. Liu, and Y.- S. Wu, Exotic electronic states in the world of flat bands: From theory to material, Chin. Phys. B **23**, 077308 (2014).

[50] G. Kresse and J. Furthmuller, Efficient iterative schemes for ab initio total-energy calculations using a plane-wave basis set, Phys. Rev. B **54**, 11169 (1996).

[51] J. P. Perdew, K. Burke, and M. Ernzerhof, Generalized Gradient Approximation Made Simple, Phys. Rev. Lett. **77**, 3865 (1996).

[52] M. Bukov, L. D'Alessio, and A. Polkovnikov, Universal high-frequency behavior of periodically driven systems: From dynamical stabilization to Floquet engineering, Adv. Phys. **64**, 139 (2015).

[53] R. Dong, M. Pfeffermann, H. Liang, Z. Zheng, X. Zhu, J. Zhang, and X. Feng, Large-area, free-standing, two-dimensional supramolecular polymer single-layer sheets for highly efficient electrocatalytic hydrogen evolution, Angew. Chem. Int. Ed. **54**, 12058 (2015).

[54] C. H. Lee, M. Claassen, and R. Thomale, Band structure engineering of ideal fractional Chern insulators, Phys. Rev. B **96**, 165150 (2017).

[55] R. Morf and B. I. Halperin, Monte Carlo evaluation of trial wavefunctions for the fractional quantized Hall effect: Spherical geometry, Z. Phys. B **68**, 391 (1987).

[56] Q. Niu, D. J. Thouless, and Y. S. Wu, Quantized Hall conductance as a topological invariant, Phys. Rev. B **31**, 3372 (1985).

[57] F. D. Haldane, Fractional Statistics in Arbitrary Dimensions: A Generalization of the Pauli Principle, Phys. Rev. Lett. **67**, 937 (1991).

[58] A. Sterdyniak, N. Regnault, and B. A. Bernevig, Extracting Excitations from Model State Entanglement, Phys. Rev. Lett. **106**, 100405 (2011).

[59] F. Mahmood, C.- K. Chan, Z. Alpichshev, D. Gardner, Y. Lee, P. A. Lee, and N. Gedik, Selective scattering between Floquet–Bloch and Volkov states in a topological insulator, Nat. Phys. **12**, 306 (2016).

[60] E. J. Sie, J. W. McIver, Y. H. Lee, L. Fu, J. Kong, and N. Gedik, Valley-selective optical Stark effect in monolayer WS2, Nat. Mater. **14**, 290 (2015).

[61] E. J. Sie, C. H. Lui, Y.- H. Lee, L. Fu, J. Kong, and N. Gedik, Large, valley-exclusive Bloch-Siegert shift in monolayer WS2, Science **355**, 1066 (2017).

[62] M. Zhou, W. Ming, Z. Liu, Z. Wang, Y. Yao, and F. Liu, Formation of quantum spin Hall state on Si surface and energy gap scaling with strength of spin orbit coupling, Sci. Rep. **4**, 7102 (2014).

[63] J. K. Freericks, H. R. Krishnamurthy, and T. Pruschke, Theoretical Description of Time-Resolved Photoemission Spectroscopy: Application to Pump-Probe Experiments, Phys. Rev. Lett. **102**, 136401 (2009).

[64] M. A. Sentef, M. Claassen, A. F. Kemper, B. Moritz, T. Oka, J. K. Freericks, and T. P. Devereaux, Theory of Floquet band formation and local pseudospin textures in pump-probe photoemission of graphene, Nat. Commun. **6**, 7047 (2015).

[65] A. Farrell, A. Arsenault, and T. Pereg-Barnea, Dirac cones Floquet side bands, and theory of time-resolved angle-resolved photoemission, Phys. Rev. B **94**, 155304 (2016).